Korean J. Chem. Eng., **16**(1), 96-103 (1999)

REMOVAL OF SURFACE CONTAMINANTS BY CRYOGENIC AEROSOL JETS

Cheol Nam Yoon, Hotae Kim, Sun-Geon Kim† and Byung-Hun Min*

Department of Chemical Engineering, Chung-Ang University, 221 Huksukdong, Dongjakgu, Seoul, 156-756 Korea
**Department of Chemical Engineering, The University of Suwon, Suwon P.O.Box 77, Suwon 440-600, Korea
(Received 27 July 1998 • accepted 11 November 1998)

Abstract – Removal of surface contaminants by various cryogenic aerosol jets has been experimentally investigated. Simplified theoretical consideration of their removal mechanism has been also presented based on the impact power of the aerosol jets. Under atmospheric operation, water vapor and carbon dioxide could make their particles independent of their concentrations in the carrier gas while argon and nitrogen could hardly solidify to their own particles. The cryogenic aerosol jets were very effective in removing both submicron particle contaminants and photoresist films on wafers. The rate of the PR film removal strongly depended on the hardness of the film. Molecular organic films could be also removed with the aerosol jets. In general, the removal of the contaminants depends primarily on the physical impact. The removal rate increased with the mass concentration of the aerosol particles, regardless of their nature. The rate also increased with the impact velocity of the jets which was controlled by either the chamber pressure or the distance between the nozzle tip and the contaminant surface. The cryogenic aerosol-free jet was much less effective than the corresponding aerosol jets but had some effectiveness compared to the noncryogenic one. The thermal shock of the film was, therefore, supposed to have a secondary effect on the contaminant removal.

Key words: Cryogenic Aerosol Cleaning, Low-Pressure Impactor, Particle Contaminants, Molecular Films, Photoresist, Sublimation

INTRODUCTION

Cryogenic jets have been widely used in removing dirt and contaminant films on the surfaces of semiconductor devices, precision products, printed circuit boards and machines, and in removing various coatings on surfaces, to name a few. The aerosol particles in the jets include ice, dry ice and solidified argon, all of which can be formed in a cryogenic environment and sublimed after the surface contaminants are removed. They have advantages of no waste production, the capability to clean complex-shaped objects and no need to disassemble and assemble the machines to be cleaned, over conventional dry and wet cleaning [Skidmore, 1987; Ruzillo,1990], and other abrasive blasting methods. Ohmori et al. [1989] proposed ice scrubber cleaning and discussed the qualitative nature of the process. Their original idea was improved by adding either jet-acceleration supplement [Nagae et al., 1989] to enhance the physical strength of the jets, or solutes [Endo et al., 1992] to increase the chemical solubility of the dirt on the surface. Dry ice cleaning is known to be effective in removing contaminants from precision to large-scale cleaning. Dry ice methods were initiated by Kashu et al. [1984] to remove photoresist films on wafer. Many practical patents have been issued [Williford et al., 1994; Peterson et al., 1994] and the solidified argon and nitrogen introduced as new media [McDermott et al., 1994; Wu et al., 1996]. In spite of the wide applications of the methods, however, as yet there have been few studies on the formation of aerosol particles, the removal mechanism and the comparison of the removal rates of various cryogenic jets. In this study, we have investigated how the removal rate is influenced by the nature of the source gases and the contaminants to be removed, and the process variables, such as the mass concentration of the aerosol particles, chamber pressure and nozzle-to-substrate distance. We have focussed on the formation mechanism of the cryogenic particles and their strength for the removal of various contaminants. The media investigated include ice, dry ice, argon and their combination.

†To whom correspondence should be addressed.
E-mail : sgkim@cau.ac.kr

EXPERIMENTAL SECTION

1. Cleaning Apparatus

The experimental apparatus for cryogenic aerosol cleaning is shown elsewhere [Yoon, 1997; Yoon et al., 1998]. The cryogenic heat exchanger cools down the carrier gas stream containing the source gas component, by passing liquid nitrogen through the jacket. The source gas may solidify into fine particles by phase transition. The cooled stream passes through a nozzle to expand into a low-pressure chamber and has a second chance for particle formation by further cooling. The particles in the high-velocity jet issuing from the nozzle hit the contaminated surface placed perpendicular to the jet, remove the contaminants and sublime by themselves. The substrate moves horizontally back and forth in 1 minute per cycle

with or without rotation. The rate of the horizontal movement is fixed at 0.0008 m/s, while the rotational speed is 57.5 rpm. For the rotational back-and-forth movement, the cleaned area appears as a circle whose center coincides with the half point of the whole horizontal displacement.

2. Preparation of Substrates

The contaminated surfaces were prepared by depositing ultrafine smoke particles on a slide glass and coating molecular organic film and photoresist (PR) film, respectively, on a wafer. The smoke particles were generated by a cigarette lighter with full opening of its fuel injection valve. They were deposited onto the slide glass located at 0.01 m from the lighter opening until the light transmittance of the glass immediately dropped to zero, which was checked by UV-VIS (JASCO V-550, Jasco Co.). The smoke particles deposited on the slide glass were spherical but they were agglomerated like necklaces. The number and weight average diameters were measured as 226 and 238 nm, respectively, and the distribution was found to be very narrow [Yoon, 1997].

Molecular contaminant films were formed by dissolving measured quantities of eicosane in 5 ml heptane, depositing two drops of the solution onto a clean gemanium attenuated total reflectance (ATR) plate and spreading the material across the plate to produce films of roughly equal thickness. Eicosane was chosen because it has low solubility (0.19 mole%) in liquid carbon dioxide [Hills, 1995] to exclude the solubility effect in the mechanism of the film removal.

PR (AZ1512) films with 1.2-μm thickness were formed on the wafer by a spin coater. The film was baked at 95 °C for 30 min. Twenty micrometer-thick PR films (PLP40) were also prepared to test the effect of film hardness. The PR films with different hardness were obtained without baking, and with baking at 105 °C for 212s and at 150 °C for 600s, whose average Micro Vickers hardness were 7.1, 11.07 and 27.46, respectively.

3. Process Variables for Cleaning

The flow rates and partial pressures of the source gases for various aerosol media are shown in Table 1. The media M1 was prepared by spraying water droplets with an ultrasonic vibrator at the rate of 0.1027×10^{-3} kg/min in particle-free nitrogen as a carrier gas at 25 °C. [Sung et al., 1996]. The composite media M2 and M3 were made by mixing 2×10^{-5} m^3/min of CO_2 and argon, respectively, with 0.060×10^{-3} kg/min of water vapor in nitrogen gas at 25 °C. Since the exact mass flow rates of CO_2 and argon gases corresponded to 0.0392×10^{-3} and 0.0357×10^{-3} kg/min, respectively, the total mass flow rates of the aerosol sources were 0.0992×10^{-3} and 0.0957×10^{-3} kg/min, respectively, close to the flow rate of the water droplets in M1. For the generation of pure dry ice and solidified argon particles, carbon dioxide and argon were added, respectively, at the same mass rates as above (0.0392×10^{-3} and 0.0357×10^{-3} kg/min) to dry nitrogen gas at 25°C. Those media were designated as M4 and M5, respectively. All the media from M1 to M5 were passed through the cryogenic heat exchanger. To see the cryogenic effect in removal mechanism, M5 without passing through the heat exchanger was also used for removing the same contaminants. This was designated as M6. In all cases, the total flow rate of the carrier and source gases varied according to the pressure of the cleaning chamber. The flow rate, however, saturated to about 3.2×10^{-3} m^3/min below 53 kPa [Ju et al., 1996], which is the critical pressure for the flow through the nozzle to be sonic [Smith et al., 1996].

In addition to the nature of the cleaning media described above, we chose, as the process variables, the nozzle-to-substrate distance and the pressure of the cleaning chamber. The experimental conditions are shown in Table 2. To investigate the effect of one variable on the removal rate, its value was varied while the other variables were kept at the corresponding reference values.

4. Measurement of Cleaning Efficiency

In order to quantify the removal efficiency in the smoke-particle removal, the light transmittance of the slide glass was measured with UV-VIS (JASCO V-550, Jasco Co.). We chose the measuring point at 0.006 m apart from the center of the cleaned circle, where the effect of the process variables on the efficiency best appeared.

In the case of the PR film, the removal rate or impact power was measured as the radius of the completely PR-removed area as described elsewhere [Yoon et al., 1998]. On the other hand, simply to see the effect of film hardness on the efficiency, only the reciprocating movement of the substrate was allowed and the average depth of the removed film was measured with α-step (α-200, PENCOR Instrument).

The impact on the PR film and its removal were observed with metallurgical microscope (FX-35WA, Nikon) and scan-

Table 2. Experimental conditions

Process variables	Their values chosen	
Pressure (kPa)	8.0*, 14.7, 21.3, 34.7, 48.0	
Nozzle-to-substrate distance ($\times10^{-3}$ m)	Smoke removal	5, 10*, 15
	Photoresist removal	5*, 10, 15

*reference condition

Table 1. Flow rates and partial pressures of the source gases

Cleaning media	M1	M2	M3	M4	M5	M6
Source gas	Water vapor	Water vapor+CO_2	Water vapor+argon	CO_2	Argon	Argon (Not cryogenic)
Mass flow rate ($\times10^{-3}$ kg/min)	0.1027	0.0992 (0.0600+0.0392)	0.0957 (0.0600+0.0357)	0.0392	0.0357	0.0357
Partial pressure, kPa	3.25	3.14 (1.90+1.24)	3.03 (1.90+1.13)	1.24	1.13	1.13
	98.05**	98.16**	98.27**	100.06**	100.17**	100.17**

*Under maximum carrier gas flow rate.

**Nitrogen partial pressure.

ning electron microscope (JSM-5200, JEOL Co.), respectively.

5. Theoretical Consideration of Cleaning Power

The physical cleaning power P is given as the product of the particle flux and the kinetic energy of single particle:

$$P = (N_p v_p)\frac{1}{2} m_p v_p^2 = N_p \frac{1}{2}\left(\frac{\pi d_p^3 \rho_p}{6}\right) v_p^3 = \frac{1}{2} M_p v_p^3 \quad (1)$$

where N_p is the number concentration, v_p the impact velocity, m_p the mass, d_p the diameter, ρ_p the density and M_p the mass concentration of the cleaning particle.

6. Particle Formation in Cryogenic Heat Exchanger

The particle (droplet) formation depends on the supersaturation of the source gas. The birth of the particles begins with the formation of the critical nuclei, whose rate is highly dependent on the saturation ratio of the gas [Friedlander, 1977]. Subsequent particle growth occurs by the condensation of the source-gas molecules which have not participated in the nucleation. When the particles already exist in the system, the gas molecules may either self-nucleate or condense out on the existing particles, depending on the concentration of the particles and the saturation ratio of the gas [Friedlander, 1977]. Fig. 1 shows the vapor pressure data for water vapor, carbon dioxide, argon and nitrogen. The velocity and temperature fields within the heat exchanger were calculated numerically from momentum and energy balance equations by using TEACH code. The axial-velocity distributions and radial temperature of the carrier gas are shown in Figs. 2 and 3 for the inlet, middle and outlet of the exchanger. The outlet velocities of the carrier gas drop to about one-third of the inlet velocities due to the volume reduction in the cryogenic environment. At an average outlet temperature of about $-140\,^{\circ}C$, the media containing water and/or carbon dioxide (M1, M2 and M4) are supposed to solidify regardless of their concentrations (partial pressures). However, argon (M5) and nitrogen gases would not condense at all under the partial pressures given in our experiment (Table 1). As shown in Fig. 1, argon gas would condense above 26.7 kPa even though the average outlet temperature reaches the temperature of liquid nitrogen. Therefore, the media M5 are supposed to have a negligible number of particles and so act as a gas jet only.

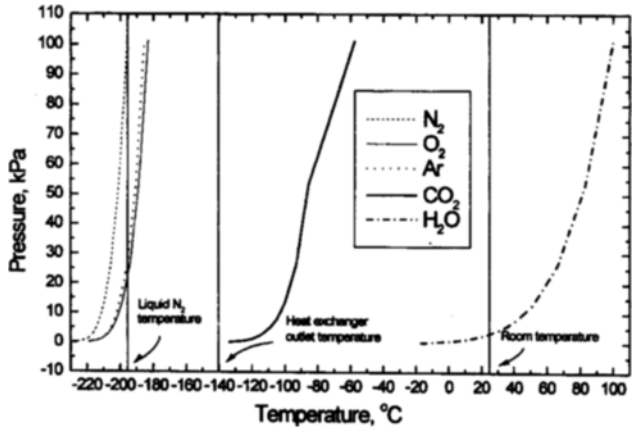

Fig. 1. Vapor pressure curves for the gases involved in our experiment.

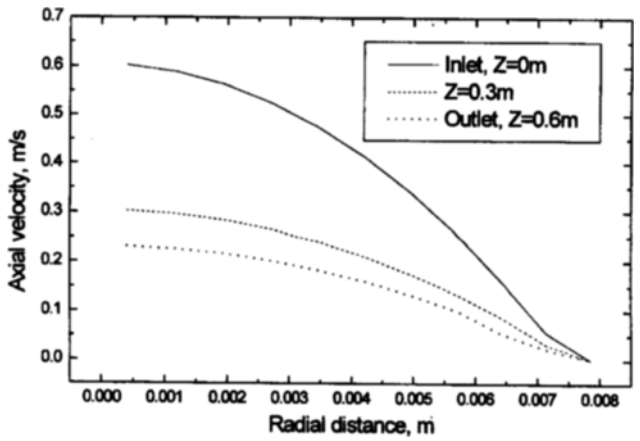

Fig. 2. Axial velocity distributions calculated by TEACH code at different distances from the heat exchanger inlet.

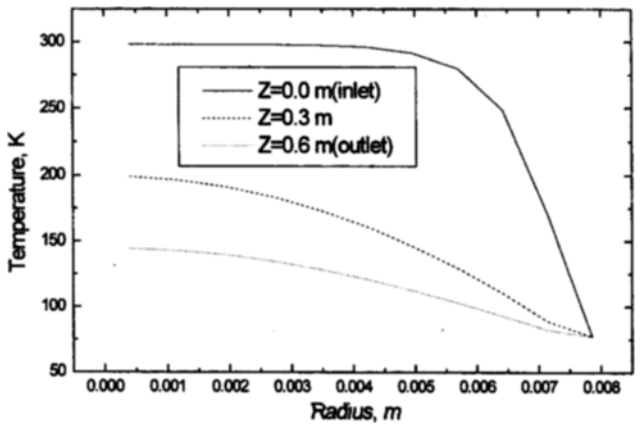

Fig. 3. Temperature distributions calculated by TEACH code at different distances from the heat exchanger inlet.

For the media M1, the droplets prepared from the ultrasonic nebulizer are supposed to be completely evaporated due to mixing with dry nitrogen gas, then completely condensed and finally solidified in the heat exchanger. When both water vapor and carbon dioxide coexist like M2, the molecules of water vapor are supposed to first nucleate to form ice particles; then carbon dioxide molecules would either condense onto the surface of the particles or self-nucleate to form their own particles during the subsequent cooling. In M3, containing water vapor and argon, only water vapor is supposed to solidify.

7. Nozzle Expansion and Impact Velocity

The last chance of solidification remains around the expansion to the low-pressure cleaning chamber through the nozzle. The process is approximately isenthalpic. The Joule-Thomson coefficient at the temperature and pressure of the nozzle upstream is, however, given at about 1 K/1.013×10^5Pa [Liley et al., 1997]. The temperature drop through the expansion is then calculated as only 0.9 K and the additional cooling is not sufficient for further solidification.

The cleaning power depends on both the mass concentration and the velocity of the cleaning media as shown in Eq. (1). The velocity of the carrier gas increases as the chamber pressure decreases and remains constant below the pressure of about 53.3 kPa as described before. The true impact veloc-

ity is determined by the inertia resulting from the velocity entering the velocity boundary layer existing near the substrate surface. The complete analysis of the cleaning power is, however, not available yet since the particle behavior near the point of impact is not known due to the complexity of the flow and temperature fields. Since a velocity boundary layer exists near the substrate surface, in order to strike the surface, the solidified particles must have a stopping distance longer than the thickness of the layer; hence their velocity [v_p in Eq. (1)] at the point of impact must be greater than zero. The situation is expressed as:

$$h = \tau v_p' \geq \delta \tag{2}$$

where h is the stopping distance of the particle, δ is the thickness of the boundary layer, v_p' is the particle velocity entering the layer, and τ is the relaxation time of the particle with the diameter d_p. τ is expressed as [Hinds, 1982]:

$$\tau = \frac{Cd_p^2\rho_p}{18\,\mu} \tag{3}$$

where C is the Cunningham slip correction factor, ρ_p the density of the particle and μ the viscosity of the carrier gas. The analysis demonstrates that the relaxation time τ, the stopping distance h and hence the impact velocity v_p all increase with the particle size. Therefore, the aerosol-free jet (M5) having only gas molecules, due to their small d_p, exhibits the shortest stopping distance, and hence the lowest cleaning power.

As the chamber pressure decreases, the nozzle-tip velocity increases; accordingly, the velocity boundary layer becomes thinner and the gas velocity entering the layer increases. These changes are stopped when the chamber pressure gets down to the critical value of 53.3 kPa, described as before. Then, the velocity v_p' no longer increases and is assumed constant regardless of the media. On the other hand, as the chamber pressure decreases, the slip correction factor increases, and hence the relaxation time and stopping distance also increase. This phenomenon results in the continuous enhancement in the impact power with the reduction of the pressure, beyond the critical pressure. However, when the pressure further decreases, the mean free path of the carrier gas and hence Knudsen number increases for a given size of the particles, and finally the particle motion gets into the free molecular regime. The increase in the correction factor then stops and so does that in the impact power.

RESULTS AND DISCUSSION

1. Removal of the Smoke Particles

Fig. 4 suggests that except with M5 and M6 the nozzle-to-substrate distance does not appreciably affect the removal efficiency in the range of 0.005 to 0.015 m, so the aerosol jets are very effective in the removal of the submicron particles. The pressure of the cleaning chamber also influences the removal efficiency as shown in Fig. 5. For all kinds of the ice-containing particles, the efficiency remains almost 100% below about 45 kPa, but above it the efficiency decreases significantly with the chamber pressure. The pressure is lower than 53.3 kPa, which is the critical pressure for the sonic jet

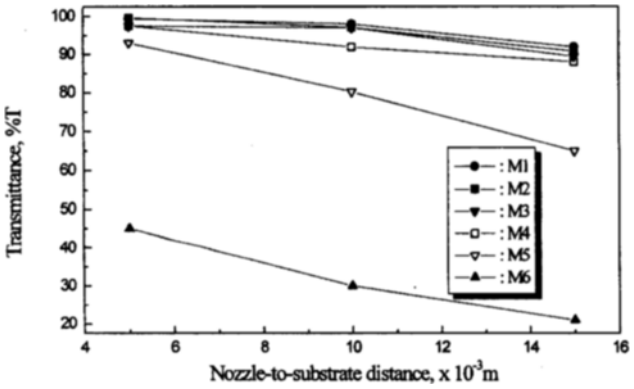

Fig. 4. Effect of nozzle-to-substrate distance on the transmittance of the contaminated slide glass for various cleaning media. Chamber pressure: 8 kPa, Number of scans: 2 times

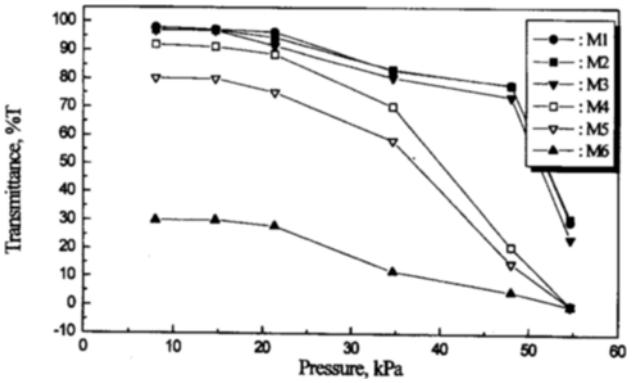

Fig. 5. Effect of the chamber pressure on the transmittance of the contaminated slide glass for various cleaning media. Nozzle-to-substrate distance: 1×10^{-2} m, Number of scans: 2 times

flow described before. However, for the dry ice (M4) and gas (M5) jets, the efficiency decreases continuously with the chamber pressure, showing no existence of such a threshold pressure. M6, which is noncryogenic without any aerosol particles, has far less efficiency than even M5. This implies that the thermal effect caused by the cryogenic jets has some effect on the removal of the contaminants [Hills, 1995].

2. Removal of Molecular Contaminant Film

Fig. 6 shows a series of infrared spectra of the clean, eicosane-contaminated germanium ATR plates and the plates cleaned with various media. In the Figure, the infrared absorption below 900 cm^{-1} is caused by the germanium plate. Fig. 1(a) shows the infrared vibrational modes of eicosane, including a very intense carbon-hydrogen stretching mode at approximately 2,920 cm^{-1}. This mode is diminished in the infrared spectra of the plate removed by all the jets for less than 1 minute. Even M5, the aerosol-free jet could remove the film entirely. However, the exact times for removal could not be measured in our experiments.

3. PR Film Removal

The SEM pictures in Fig. 7 show a series of the PR films being removed by the ice+dry ice particles (M2) in rotational scanning. It is clearly observed that the film was being scared and finally removed, which confirmed that the particles hit

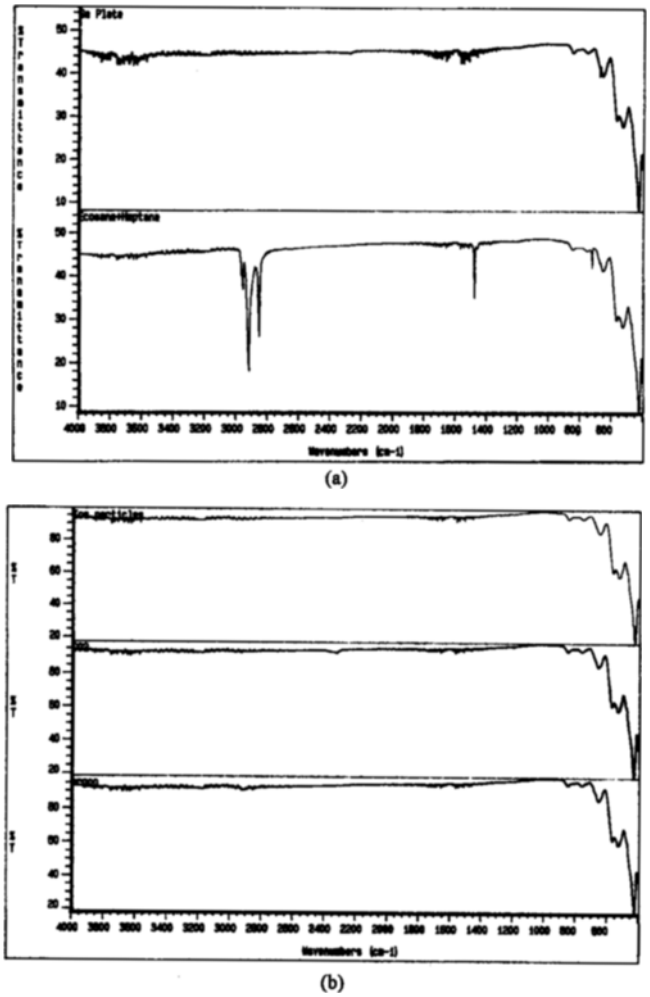

Fig. 6. Infrared multiple-reflection spectra of (a) top: clean germanium-attenuated total-reflectance plate, bottom: germanium plate covered with eicosnae, and (b) the plate removed with top: M1, middle: M4, bottom: M5.

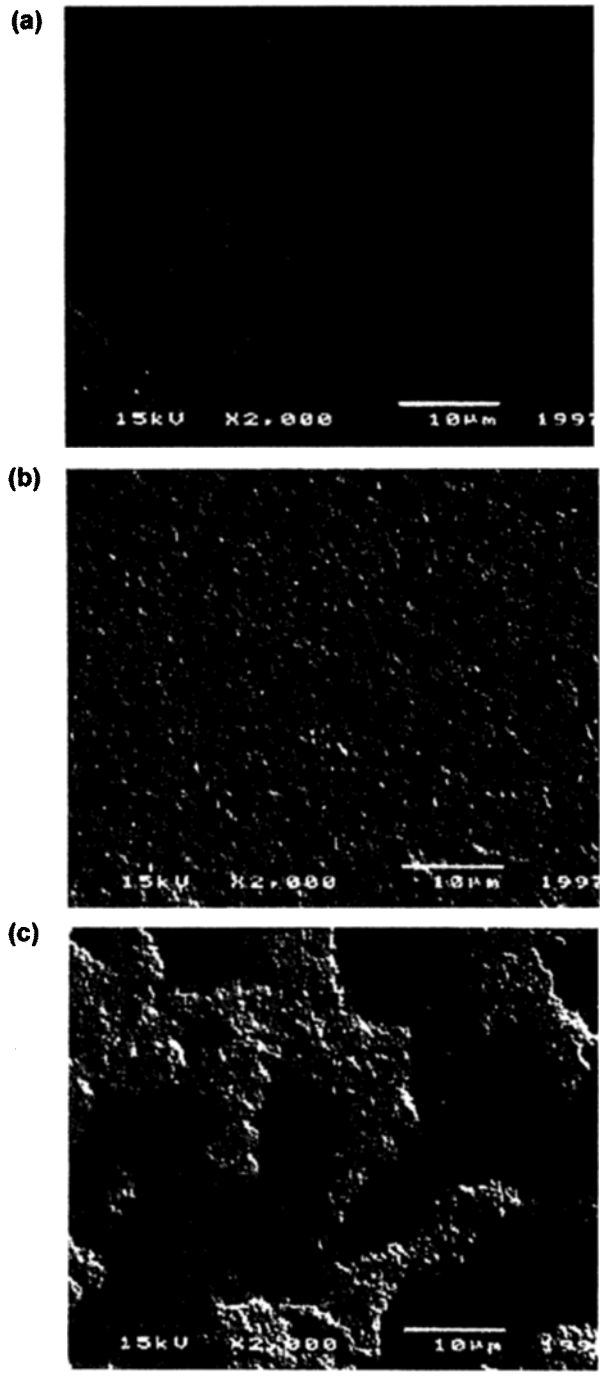

Fig. 7. SEM pictures showing the removal of PR on wafer for ice+dry ice particles (M2) under the reference condition. (a) before removal (b) at early stage of removal (c) at later stage of removal

the film surface. The fringe formation by the impact of the cryogenic jet is shown in Fig. 8 for one-point impacts by three different media. The variations in the widths of fringes and their sharpness are clearly observed, showing the descending order of the impact power as M1, M4 and M5. Clearly, M5, the aerosol-free jet also had some effect on the impact and hence the removal of the PR film, while M6, the noncryogenic jet left no mark of the film removal at all.

The effect of film hardness on the removal depth as a measure of the impact power is shown in Fig. 9. The depth decreases with the film hardness. For the film with the same hardness, the ice particle jet has the highest power while the noncryogenic gas (M6) jet has the lowest. The hardness of the film has less effect on the depth for the aerosol-free jets (M5 and M6).

The effect of the nozzle-to-substrate distance on the radius of the removed area is shown in Fig. 10. The velocity of the particles issuing from the nozzle tip decreases because the carrier gas slows down with the distance. Therefore, at the distance about 0.015 m apart from the nozzle the efficiency almost drops to zero, showing the PR removal is more difficult than the smoke-particle removal (Fig. 4).

Fig. 11 shows the effect of the chamber pressure on the impact power. As in the smoke cleaning, the powers of both pure dry ice (M4) and the gas (M5) jets just decrease continuously with the pressure, while for ice-containing media (M1, M2 and M3) it remains constant below a certain pressure and then decreases with the pressure. The pressure at which the reduction in the power occurs is different according to the nature of the surface contamination. For the PR-film removal it

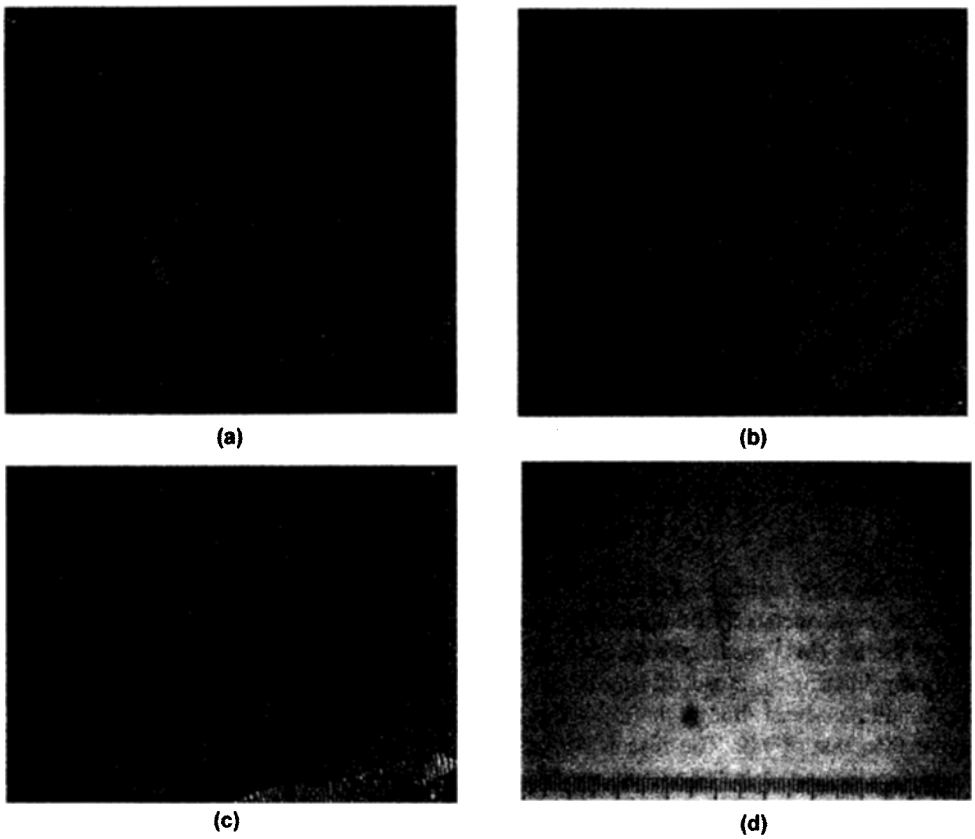

Fig. 8. Variation in the impact of various cleaning media on photoresist-covered wafer under the reference condition.
(a) Ice particles (M1), (b) dry ice particles (M4), (c) argon+nitrogen gas stream (M5), (d) noncryogenic argon+nitrogen gas stream (M6)

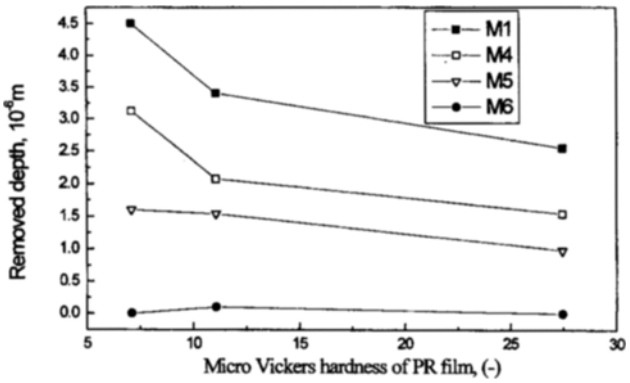

Fig. 9. The effect of the hardness of PR film on the radius of removed area under the reference condition.

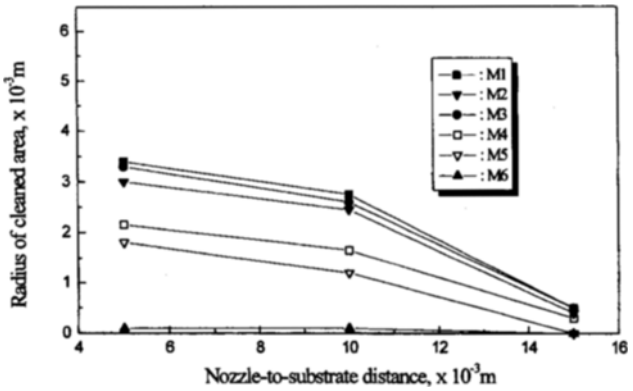

Fig. 10. Effect of nozzle-to-substrate distance on the radius of cleaned area for various cleaning media.
Chamber pressure : 8 kPa, Number of scans : 30 times

ranges between 13 and 20 kPa, depending on the media, while it was about 45 kPa in the smoke removal. This also implies that the removal of PR films is more difficult than that of smoke particles. As described before, the existence of the pressure in the PR removal is supposed to be related to the fact that the regime in particle motion changes from transition to free-molecule regime so that no further increase in the slip correction factor is expected. As noted in Eq. (3), this threshold chamber pressure increases with the particle size.

4. Comparison of Impact Powers of Various Media.

So far the media used in the jets have been found to definitely influence the impact power. The powers of the ice (M1) and ice+dry ice (M2) particles are the highest, followed by those of M3, pure dry ice (M4) and M5 in turn. In any case, M6 has the lowest impact power. As described before, argon and nitrogen cannot solidify under our experimental conditions, so M3 contains ice particles and nitrogen plus argon gas, and M5 consists of nitrogen plus argon gas with no particles. The impact power is estimated as in Eq. (1). The order in the power in our results is the same as that of the mass concentration of the source gases, since the concentration determines the particle size and this in turn fixes the impact velocity. The expansion through the nozzle is supposed to give no chance for

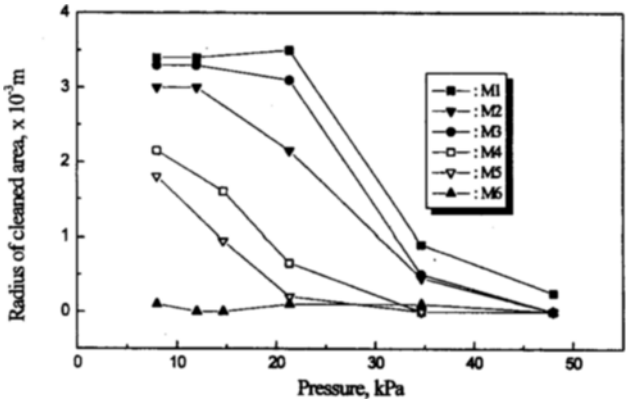

Fig. 11. Effect of the chamber pressure on the radius of cleaned area for various cleaning media.
Nozzle-to-substrate distance: 0.5×10^{-2} m, Number of scans: 30 times

additional formation of the cleaning particles as described before, but merely contributes the acceleration of the particles.

The impact powers of the ice (M1) particles have been always close to, but slightly inferior to, those of ice+dry ice (M2) under the same conditions, even though the mass flux of M1 is slightly higher than that of M2. The reason is that some water often caused the clogging of the nozzle tip, making the actual efficiency drop. Instead, as in M2, the partial replacement of water with carbon dioxide vapor reduces the trouble. The combination of carbon dioxide and water vapor first generates the ice particles which are more condensable, and the subsequent condensation of carbon dioxide molecules onto their surface. If there is only carbon dioxide in the carrier gas (nitrogen) (M4), its self-nucleation occurs to yield pure dry-ice particles. The fact that the impact power of M2 is close to that of M1 tells us that the mass concentration and impact velocity of M2 particles are similar to those of M1 particles. This implies that the particle sizes are similar in both media. It is, therefore, confirmed that the particle formations actually occur by almost the same routes in these media, which has been already postulated as before. In M3, water vapor is supposed to take part in the particle formation while argon remains in the gas phase. The average size of the particles is then expected to be smaller than either M1 or M2. In M4, the dry ice particles nucleate by themselves with much smaller mass flux, having appreciably lower impact power as shown in the figures above. In our results, M5, the aerosol-free jet, has lower power than that of M4, but has higher power than M6, the noncryogenic jet. This means that the cryogenic effect play a certain role in removing the contaminants.

CONCLUSIONS

We have investigated the effect of the aerosol media prepared by different source gases, the process variables, and the source of contamination on the impact power. From our study we have concluded:

1. At atmospheric pressure, water vapor and carbon dioxide solidified in the cryogenic heat exchanger regardless of their concentrations in the carrier gas, while the solidification of argon gas required partial pressures far above 26.7 kPa.

2. In cryogenic jet cleaning the removal mechanism of the contaminants mainly depended on the physical impact of the jet. The aerosol jets were, therefore, more effective in the contaminant removal than the aerosol-free gas jet, due to the inertia effect of the aerosol particles. Cryogenic aerosol cleaning was very effective in the removal of submicron particles and the photoresist films, the rates of which depended on the film hardness. The molecular organic film could be removed with the cryogenic jets with or without the aerosol particles.

3. The cryogenic aerosol-free jet had also some limited power for the contaminant removal, which showed evidence of the thermal-shock effect in the removal mechanism.

4. The order of the media in the impact power was the same as that of the mass concentration of the condensable source gases, since the concentration determined the particle size and this in turn fixed the impact velocity.

5. The impact velocity increases with the reductions of the chamber pressure and nozzle-to-substrate distance and so does the impact power. For the aerosol jets, there existed a threshold chamber pressure below which the power saturated. The pressure increased with the particle size.

ACKNOWLEDGEMENT

This work was supported by the Ministry of Education through Interuniversity Semiconductor Research Center (97-158) in Seoul National University. The authors also thank the Center for Environmental and Clean Technologies in the University of Suwon (98-A4).

REFERENCES

Endo, S., Ohmori, T., Fukumoto, T. and Namba, K., "Method of Treating Surface of Substrate with Ice Particles and Hydrogen Peroxide," US Patent 5081068, 1992.

Friedlander, S.K., "Smoke, Dust and Haze," John-Wiley & Sons, New York, 248 (1977).

Hills, M.M., "Carbon Dioxide Jet Spray Cleaning of Molecular Contaminants," *J. Vac. Sci. Technol. A*, **13**, 30, Jan/Feb (1995).

Hinds, W.C., "Aerosol Technology," John-Wiley & Sons, New York, 105 (1982).

Ju, D.U., Chung, J.H. and Kim, S.G., "Surface Cleaning by Ice Particle Jet(I)," *HWAHAK KONGHAK*, **34**, 346 (1996).

Kashu, S., Fuchita, E., Manabe, T. and Hayashi, C., "Deposition of Ultra Fine Particles Using a Gas Jet," *Jap. J. Appl. Phys.*, **23**, L910 (1984).

McDermott, W.T., Ockovic, R.C., Wu, J.J., Cooper, D.W., Schwarz, A. and Wolfe, H.L., "Surface Cleaning Using an Argon or Nitrogen Aerosol," US Patent 5294261, 1994.

Nagae, A., Satou, S., Fukumoto, T. and Ohmori, T., "Incliding Lattice Defect with Ice Particles in Semiconductor Wafer," US Patent 4820650, 1989.

Ohmori, T., Fukumoto, T., Kato, T., Tada, M. and Kawakuchi, T., "Ultra Clean Ice Scrubber Cleaning with Jetting Fine Ice Particles," Semiconductor Cleaning Technology/1989, Ruzyllo,

J. and Novak, R. E., eds., Electronics and Dielectrics and Insulation Divisions Proceedings Vol 90-9, The Electrochemical Society, Inc., Pennington (1990).

Liley, P. E., Thomson, G. H., Friend, D. G., Daubert, T. E. and Buck, E., "Physical and Chemical Data, 2-135", Perry's Chemical Engineers' Handbook, 7th ed., Ed. by Perry, R. H. and Green, D. W. (1997).

Peterson, R. V. and Krone-Schmidt, W., "System for Precision Cleaning by Jet Spray", US Patent 5315793 (1994).

Ruzyllo, J., "Issues in Dry Cleaning of Silicon Wafers", *Solid State Technology*, S1, Mar. (1990).

Skidmore, K., "Cleaning Techniques for Wafer Surfaces", *Semiconductor International*, 81, August (1987).

Smith, J. M. and Van Ness, H. C., "Introduction to Chemical Engineering Thermodynamics", McGraw-Hill, New York (1987).

Williford Jr., J. F., "The Method for Removing Particulate Matter", US Patent 5364474, 1994.

Wu, J. J., Syverson, D., Wagener, T. and Weygand, J., "Wafer Cleaning with Cryogenic Argon Aerosols", *Semiconductor Intern.*, 113 (1996).

Yoon, C. N., "Surface Cleaning Process Using Sublimable Solid Particle Jet", M.S. Thesis, Chung Ang University (1997).

Yoon, C. N., Kim, S.-G. and Min, B.-H., "The Effect of Aerosol Sources on the Cleaning Efficiency in Cryogenic Aerosol Cleaning", Submitted to I&EC, Research (1998).